EPJ Web of Conferences **28**, 06003 (2012)
DOI: 10.1051/epjconf/20122806003

Di-boson results at ATLAS

Pierre-François Giraud[a] On behalf of the ATLAS Collaboration

DSM/IRFU (Institut de Recherches sur les Lois Fondamentales de l'Univers), CEA Saclay (Commissariat à l'Energie Atomique), Gif-sur-Yvette, France

Abstract. Pairs of gauge boson produced in proton-proton collisions at a center-of-mass energy $\sqrt{s}$ of 7 TeV are reconstructed with the ATLAS detector in their leptonic final states. Based on samples of integrated luminosity $\mathcal{L} = 1.0$ fb^{-1} (for WW, WZ and ZZ) and 35 pb^{-1} (for $W\gamma$ and $Z\gamma$) of 2011 and 2010 LHC data, the total di-boson production cross sections are measured. They are found, together with the kinematic distributions of the selected di-boson systems to be compatible with the expectation from the Standard Model. The di-boson production also gives a handle on possible anomalous triple gauge boson couplings, for which 95% confidence limits are set.

ATL-PHYS-PROC-2012-018
23 January 2012

1 Introduction

In the Standard Model (SM), the triple gauge boson couplings (TGCs) are fully constraint by the electroweak symmetry. In particular, the ZZZ, $ZZ\gamma$ and $Z\gamma\gamma$ neutral TGC vertices are are absent, whereas the WWZ and $WW\gamma$ vertices are predicted non-zero. For this reason, the measurement of the di-boson final states at the LHC provides an important test of the SM: beyond Standard Model physics could contribute to the TGCs and result in modified di-boson cross sections or final state kinematics. Furthermore, non-resonant di-boson productions are a background to the search for the Higgs boson, so it is essential to understand their detection sensitivity.

This note presents measurements of the di-boson production in proton-proton collisions at a center-of-mass energy $\sqrt{s}$ of 7 TeV, with the ATLAS experiment [1]: their production cross sections are measured, and first limits on anomalous triple gauge boson couplings (aTGCs) are set. A sample of integrated luminosity $\mathcal{L} = 1.0$ fb^{-1} of 2011 LHC data was used to measure the ZZ, WZ and WW final states, and $\mathcal{L} = 35$ pb^{-1} of 2010 data for the $Z\gamma$ and $W\gamma$ final states. Presently, the only decay modes used to reconstruct these final states are $Z \to ll$ and $W \to l\nu$ (with $l = e$ or μ): the branching fractions are small, but the experimental signatures are clean.

2 Electrons, muons and photons

One of the important categories of backgrounds of the analyses presented in this note is arising from the QCD processes: a jet may produce a fake prompt lepton or photon signal. For example, pions may be mis-identified as electrons or photons. Another example is heavy flavour jets, which may result in real leptons in the final state. The main tools to reject this background are cuts on the lepton and photon identification quantities provided by the detector, which may be tightened if necessary, and cuts on the isolation energy (the sum of the transverse energies measured by the calorimeter or the inner detector, in a cone of fixed size around the candidate lepton or photon).

The probability that particles from jets pass the lepton and photon identification and isolation cuts is so small that it would be both impractical and inaccurate to estimate this background with Monte-Carlo (MC) simulation. Instead, the analyses presented in this note rely on a data-driven method.

A control region enriched in events from the QCD process is built using the full selection of the chosen final state, except that the isolation or identification cuts are reversed. The event yield observed in the control region is extrapolated to the signal region, by the use of a fake factor. The fake factor needs to be estimated in an independent QCD control sample: for example a sample of di-jet triggered events, or, if available, a sample obtained by reversing another of the analysis cuts.

The estimation of this fake factor is in general a significant source of systematic error: in particular the fake factor varies with data taking conditions (instantaneous luminosity and pile-up), and the control region may inaccurately describe the jet content of the signal region (heavy to light jet ratio for example).

3 $WW \to l\nu l\nu$

The $WW \to l\nu l\nu$ signal is measured in final states with two leptons and missing transverse energy ($E_{\mathrm{T}}^{\mathrm{miss}}$) [2]. Background discrimination and estimation is challenging as several processes may fake this final state, either because they contain real leptons and $E_{\mathrm{T}}^{\mathrm{miss}}$(top events, discriminated by a jet veto), or fake $E_{\mathrm{T}}^{\mathrm{miss}}$(Drell-Yan, discriminated with dilepton mass veto and tight $E_{\mathrm{T}}^{\mathrm{miss}}$cut) or jets misidentified as prompt leptons (W + jet events, discriminated with tight lepton identification and isolation cuts). After applying a tight selection, 414 events are observed in a sample of integrated luminosity $\mathcal{L} = 1.0$ fb^{-1}, for a total estimated background of $169.8 \pm 6.4(\mathrm{stat.}) \pm 27.1(\mathrm{syst.})$ events, determined with a combination of data-driven and MC techniques. The dominant systematics are coming from the background es-

[a] e-mail: pierre-francois.giraud@cea.fr

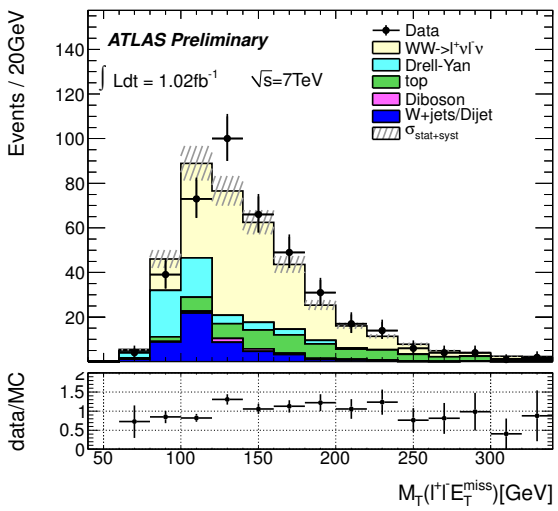

Fig. 1. Distribution of the transverse mass of the di-lepton plus missing transverse energy system for WW candidates. The points are the data and the stacked histograms are from MC predictions except the W+jets background, which is obtained from data-driven methods. The estimated uncertainties are shown as the hatched bands.

timation: the uncertainty arising from the jet veto, and from the fake prompt lepton estimation.

Figure 1 presents the distribution of the transverse mass of the di-lepton plus $E_{\mathrm{T}}^{\mathrm{miss}}$system after selection: no significant deviation from the SM expectation is observed. The event yield is converted to the total cross section $\sigma(pp \to WW) = 48.2 \pm 4.0(\mathrm{stat.}) \pm 6.4(\mathrm{syst.}) \pm 1.8(\mathrm{lumi.})$ pb, which is compatible with the SM prediction at next-to-leading order (NLO) of 46 ± 3 pb.

4 $WZ \to lvll$

WZ candidates are selected from events containing three isolated leptons (e or μ) and missing transverse energy [3], where two of the leptons have a corresponding invariant mass compatible with an on-shell Z decay. In comparison with the WW analysis, the WZ analysis benefits from a three-lepton requirement which reduces most of the background. For that reason, and in order to increase the analysis acceptance, slightly looser lepton requirements are applied for the leptons making the Z candidate than for the one entering the W. After selection, a total of 71 events are observed in a sample of integrated luminosity $\mathcal{L} = 1.0\ \mathrm{fb}^{-1}$. The total estimated background is of $10.5^{+3.0}_{-2.2}$ events, composed of Z+jet and top events with a jet mis-identified as a lepton (estimated with a data-driven technique), and $ZZ \to llll$ (estimated from the MC).

Figure 2 shows the distribution of the transverse mass of the three leptons plus $E_{\mathrm{T}}^{\mathrm{miss}}$system after selection. The distribution is compatible with the expectation from the SM. The event yield is converted to the cross section $\sigma(pp \to WZ) = 21.1^{+3.1}_{-2.8}(\mathrm{stat.}) \pm 1.2(\mathrm{syst.})^{+0.9}_{-0.8}(\mathrm{lumi.})$ pb, compatible with SM prediction at NLO of $17.2^{+1.2}_{-0.8}$ pb.

WZ events are additionally used to research for possible aTGC terms. Expressions for the most general effective Lagrangian for a TGC vertex may be found in [4] and [5]. Three terms of this effective lagrangian describing aTGCs

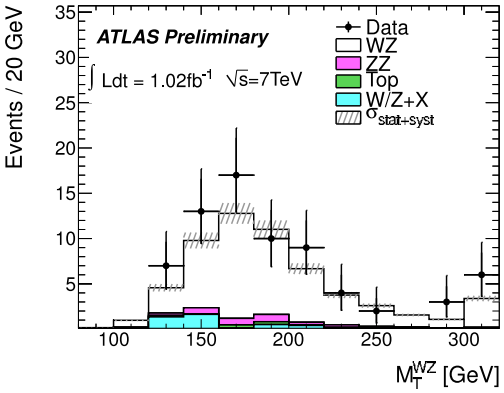

Fig. 2. Distribution of the transverse mass of the WZ system after all cuts have been applied. The points represent observed event counts with statistical errors, whereas the stacked histograms are the predictions from simulation including the statistical and systematic uncertainty. The last bin is an overflow bin.

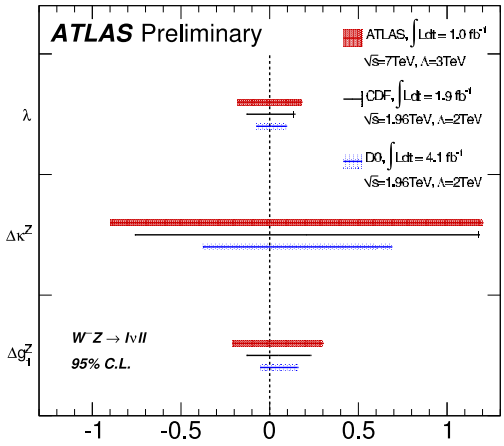

Fig. 3. Limits on aTGC from ATLAS and Tevatron experiments. CDF [6] and D0 [7] limits are for WZ production with a $p_{\mathrm{T}}(Z)$ shape fit; ATLAS limits are for a cross section fit. Luminosities, centre-of-mass energy and cut-off Λ for each experiment are shown and the limits are for 95% C.I.

are presently accessible with the ATLAS WZ data: λ, $\Delta\kappa^Z$ and Δg_1^Z. The WZ cross-section measurement is used to determine 95% frequentist confidence intervals on these three terms, which are shown in figure 3, and are compared to Tevatron limits. The limits set by ATLAS are compatible with those of Tevatron, which have the best sensitivity at the moment. In the future, ATLAS will use the information in the kinematic distributions of the WZ system to improve these limits.

5 $ZZ \to llll$

The researched signature for the ZZ signal [8] is events containing two pairs of isolated leptons (e or μ), compatible with on-shell Z decays. Events with four leptons at the LHC are extremely rare, making the ZZ analysis effectively background free. A total of twelve events are observed for an integrated luminosity $\mathcal{L} = 1.0\ \mathrm{fb}^{-1}$. The backgrounds considered in this analysis are inclusively events $lllj$ or $lljj$, where j is a jet mis-identified as a lepton (such final states may be found in top and Z + jet events). Most of these events are rejected by the isolation requirement. A

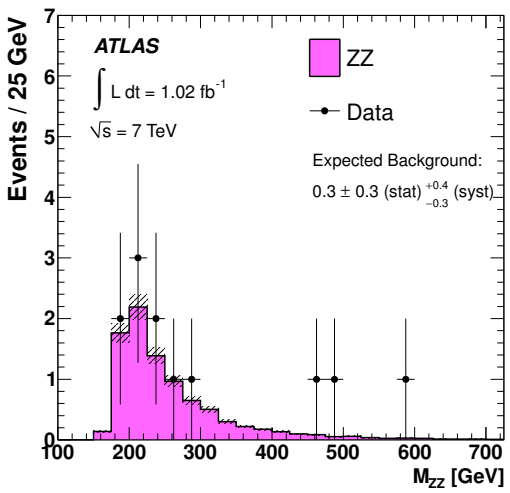

Fig. 4. Invariant mass of the four-lepton system for the selected ZZ events. The points represent the observed data and the histograms show the signal prediction from simulation. The shaded band on each histogram shows the combined statistical and systematic uncertainty on the signal prediction. The predicted number of background events from the data-driven background estimate is indicated on the plot.

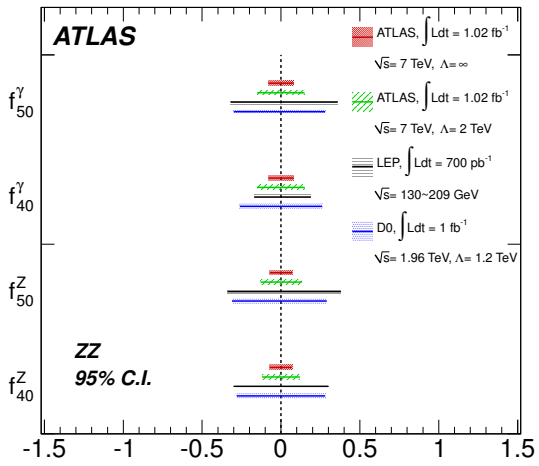

Fig. 5. Anomalous neutral TGC 95% confidence intervals from ATLAS, LEP [9] and Tevatron [10] experiments. Luminosities, centre-of-mass energy and cut-off Λ for each experiment are shown.

data-driven technique is used to estimate this background and results in $0.3 \pm 0.3(\text{stat.})^{+0.4}_{-0.3}(\text{syst.})$ events.

Figure 4 presents the invariant mass distribution of the four-lepton system after selection. Although three events are observed at an invariant mass $M_{ZZ} > 400$ GeV, the distribution is estimated to be compatible with the SM expectation. The event yield is used to estimate the total cross section $\sigma(pp \to ZZ) = 8.5^{+2.7}_{-2.3}(\text{stat.})^{+0.4}_{-0.3}(\text{syst.})\pm 0.3(\text{lumi.})$ pb, consistent with the SM prediction at NLO of $6.5^{+0.3}_{-0.2}$ pb.

Similarly to the WZ analysis, possible aTGC terms are researched using the selected ZZ event yield. In the general effective lagrangian, four aTGC vertices are accessible in ATLAS ZZ data: f^Z_{40}, f^Z_{50}, f^γ_{40} and f^γ_{50}. 95% frequentist confidence intervals are set on these four terms and are presented in figure 5. The limits set by ATLAS for neutral TGC terms are compatible, and exceed in precision, the limits set by previous experiments from LEP and Tevatron.

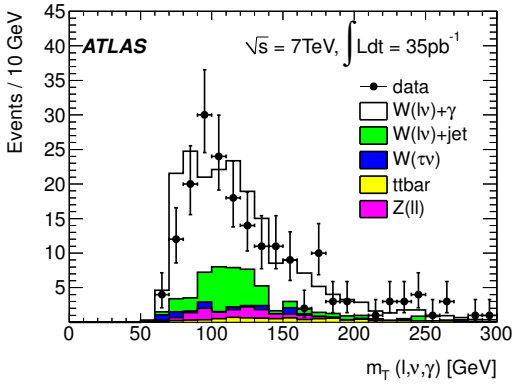

Fig. 6. Distributions for the combined electron and muon decay channels of the three body transverse mass ($m_T(l, \nu, \gamma)$) of the $W\gamma$ candidate events. MC predictions for signal and backgrounds are also shown.

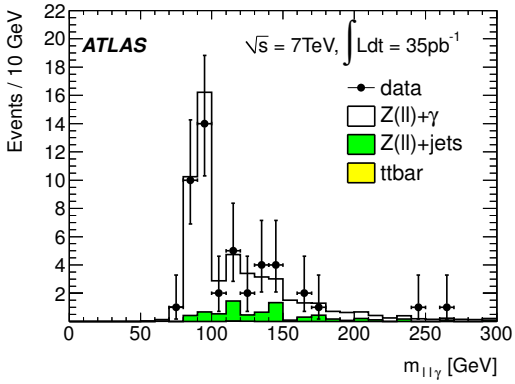

Fig. 7. Three body invariant mass $m(l^+, l^-, \gamma)$ distribution for $Z\gamma$ data candidate events. MC predictions for signal and backgrounds are also shown. Both the electron and muon decay channels are included.

6 $W\gamma \to l\nu\gamma$ and $Z\gamma \to ll\gamma$

The researched signals $W\gamma$ and $Z\gamma$ contain a leptonic W or Z candidate, and a highly energetic photon [11]. The signal is defined with phase space cuts on the photon energy ($E^\gamma_T > 15$ GeV), separation from closest lepton ($\Delta R > 0.7$), and isolation at parton level ($\sum_{\text{parton}} E_T(\Delta R < 0.4)/E^\gamma_T < 0.5$). With these cuts, 8% of the signal comes from photons originating from the fragmentation process, and no effort is made to disentangle them from the photon production of the hard process.

An integrated luminosity of $\mathcal{L} = 35$ pb^{-1} of 2010 LHC data is analysed and results in 192 $W\gamma$ candidates and 48 $Z\gamma$ candidates. The background is estimated with a data-driven technique and accounts for $\sim 29\%$ of the $W\gamma$ selection and $\sim 15\%$ of the $Z\gamma$ selection.

Figure 6 presents the distribution of the transverse mass of the $l\nu\gamma$ system for the selected $W\gamma$ candidates, and fig-

ure 7 the invariant mass of the $ll\gamma$ system for the $Z\gamma$ candidates. The kinematic distributions are compatible with the expectation from the SM. The event yields are converted to cross section measurements after background subtraction. For $W\gamma$, the cross section is measured $\sigma(pp \to W\gamma \to l\nu\gamma) = 36.0 \pm 3.6(\text{stat.}) \pm 6.2(\text{syst.}) \pm 1.2(\text{lumi.})$ pb, for a SM prediction at NLO of 36.0 ± 2.3 pb. For $Z\gamma$, the measurement is $\sigma(pp \to Z\gamma \to ll\gamma) = 6.5 \pm 1.2(\text{stat.}) \pm 1.7(\text{syst.}) \pm 0.2(\text{lumi.})$ pb, for a SM prediction of 6.9 ± 0.5. Both cross sections are compatible with the SM expectation.

7 Conclusion

Measurements of the production cross sections $pp \to WW$, $pp \to WZ$, $pp \to ZZ$, $pp \to W\gamma$ and $pp \to Z\gamma$ have been performed with the ATLAS detector at $\sqrt{s} = 7$ TeV center-of-mass energy, using samples of 1.0 fb^{-1} and 35 pb^{-1} of 2011 and 2010 LHC data. The total production cross sections are compatible with the SM predictions, and the kinematic distributions of the various di-boson systems do not show evidence of new physics. Since the di-boson production is sensitive to the predicted three-boson coupling of the Standard Model, two of the di-boson measurements (WZ and ZZ) have been used to set first ATLAS limits on possible anomalous TGC terms.

References

1. ATLAS Collaboration, JINST 3, S08003 (2008)
2. ATLAS Collaboration, ATLAS-CONF-2011-110 (2011) https://cdsweb.cern.ch/record/1373412
3. ATLAS Collaboration, ATLAS-CONF-2011-099 (2011) https://cdsweb.cern.ch/record/1369214
4. K. Hagiwara *et al.*, Nucl. Phys. B282 (1987) 253
5. J. Ellison *et al.*, Ann. Rev. Nucl. Part. Sci. 48 (1998) 33
6. CDF Collaboration, http://www-cdf.fnal.gov/physics/ewk/2008/WZatgc/
7. D0 Collaboration, Phys. Lett. B695 (2011) 67
8. ATLAS Collaboration, arXiv:1110.5016 [hep-ex] (2011), accepted by Phys. Rev. Lett.
9. LEP Collaborations, arXiv:hep-ex/0612034v2 (2006)
10. D0 Collaboration, Phys. Rev. Lett. 100 (2008) 131801
11. ATLAS Collaboration, JHEP 09 (2011) 072